NSS

Neutrosophic Sets and Systems, Vol. 60, 2023

University of New Mexico

A membership based neutrosophic approach for supervised fingerprint image classification

Vinoth D[1], and Ezhilmaran Devarasan[2,*]

Department of Mathematics, School of Advanced Sciences, Vellore Institute of Technology, Vellore.

[1]vinov002@gmail.com

[2]ezhil.devarasan@yahoo.com

*Correspondence: ezhil.devarasan@yahoo.com

Abstract. The Neutrosophic Sets (NS) mathematical model is a sophisticated paradigm that effectively addresses uncertainty. This article provides four different methods for the extraction of visual features. The proposal has been investigated with regard to both neutrosophic sets and single-valued NS. The article primarily examines two distinct features: binary and self-intensity approaches. Following that, an attempt was made to classify the images using machine learning techniques. The main objective of this article was exclusively on supervised classification algorithms. The classification of images was performed by using Decision Tree (DT), Random Forest (RF), K Nearest Neighbour (KNN),Naive Bayes (NB), and Logistic Regression (LR) algorithms. Since we have an interest in biometric images, the fingerprint image dataset was chosen for classification. The methods proposed in that research are known to as Membership Based Neutrosophic Binary Image ($MBNI_B$), Membership Based Neutrosophic Self Intensity Image ($MBNI_{SI}$), Membership Based Single Valued Neutrosophic Binary Image ($MBSVNI_B$), and Membership Based Single Valued Neutrosophic Self Intensity Image ($MBSVNI_{SI}$). The proposal possesses a range of improvement accuracy ranging from 5% to 58%.

Keywords: Machine learning; decision tree; random forest; KNN; Naive Bayes; logistic regression; neutrosophic image; fingerprint image

1. Introduction

Zadeh introduced the concept of the fuzzy set as a technique of addressing factors characterized by uncertainty. The fuzzy set employs a membership function that assigns a membership value ranging from 0 to 1 to each component of the set. Atanssov is recognized with the development of the intuitionistic fuzzy set, a mathematical system that assigns both membership and non-membership functions to each element in an existing state. Consequently, it is possible

to characterize it in a more precise and definitive way compared to a vague set. Nevertheless, the system's capacity is limited to processing incomplete and uncertain data, rendering it incapable of effectively managing the conflicting data that commonly arises in real-world scenarios. The NS, developed by Smarandache, introduces an innovative structure for addressing uncertainty by assigning memberships to truth, indeterminacy, and falsity. This pioneering invention represents a significant advancement in the field. In contrast to the intuitionistic fuzzy set, it possesses a greater capacity to effectively represent indeterminate or uncertain data. The NS has received significant attention from scholars, and its applications have been incorporated in several domains such as aggregation operators, decision-making, image processing, information measures, graph theory, and algebraic structures. In view of this expansion, we present a comprehensive overview of NS in order to offer a comprehensive understanding of the various concepts, methodologies, and developments related to their extensions. Based on the research findings, it has been observed that several developing countries, like India, China, and Turkey, are actively engaged in the exploration and study of NS. The NS has garnered significant attention from scholars due to its ability to encompass a wide range of descriptive cases. The fuzzy appearance of the neutrosophic scope is more effectively managed by this novel set. Considering the fact that study pertaining to the subject of neutrosophic has been continuing for a span of two decades and is currently garnering the attention of researchers, it is imperative that we adopt a comprehensive perspective in order to identify any prevailing patterns of thought or scientific advancements within the realm of neutrosophic research. In the context of this article, it is important to note that the fundamental definitions of NS, single valued NS and image features [1–3] are regarded as introductory.

The remainder of the paper is organized as follows. Some remarkable related works are indicated in section 2. Then in the section 3 we discussed the some preliminaries and proposed methods. The section 4 explains the implementation of proposed methods in fingerprint datasets. Finally the section 5 concludes the research findings and feature scope of the proposed methods.

List of Symbols and Abbreviations

NS**:** Neutrosophic Sets
DT**:** Decision Tree
RF**:** Random Forest
KNN**:** K Nearest Neighbour
LR**:** Logistic Regression
NB**:** Naive Bayes
SVM**:** Support Vector Machine

CNN**:** Convolutional Neural Network

$MBNI_B$**:** Membership Based Neutrosophic Binary Image

$MBNI_{SI}$**:** Membership Based Neutrosophic Self Intensity Image

$MBSVNI_B$**:** Membership Based Single Valued Neutrosophic Binary Image

$MBSVNI_{SI}$**:** Membership Based Single Valued Neutrosophic Self Intensity Image

$\mathcal{L}$**:** Maximum pixel range 2^8

P_{k_0}**:** Image padding

g_μ**:** Mean function

g_σ**:** Standard deviation function

g_λ**:** Maximum function

$\mathbb{Z}^+$**:** Positive integer

Θ_A**:** Parameter function

ξ_A**:** Cardinal of Θ_A

2. **Related works**

The study proposed by the Abdel et al. [4] categorizes 52% of the risks related to real-world data oil, gas, and coal analysis as high risks, 36% as medium risks, and 12% as usual risks throughout every aspect. The paper exhibits the significant efficacy of the neutrosophic technique in the realm of energy analysis. The utilization of neutrosophic statistical concepts is used by Afzal et al. [5] within the domain of LCR meters. The paper provides an in-depth analysis of the correlation between resistance and capacitance through the utilization of NS at particular intervals. The article presents a notable outcome of $30.18 + 40.92IN$, where IN is within the range of [0, 0.26]. Sampling provides the fundamental component of the quick-switching system. Uma et al. [6] utilized a NS-based Poisson distribution and performed a comparative analysis with a fuzzy Poisson distribution using operational characteristic curves. The probability assigned by the suggested model to a set of 1200 samples is 0.45. The automated technique of identifying individuals by evaluating their behavioral and biological characteristics is referred to as biometric recognition. Recognition and verification are two biometric processes utilized to determine an individual's distinct characteristics. A finger knuckle print feature extraction approach, an entropy-based pattern histogram, and a collection of statistical texture features, according to Heidari et al. [7], could be applied to determine how unique a person is. When these approaches were applied to the Poly-U finger knuckle print and finger knuckle print datasets, there was a significant improvement in performance, with increases of 94.91% and 98.5%, respectively. Mohammed et al. [8] applied a watermark recognition technique in their research to secure the confidentiality of patient's healthcare information by implementing a biometric system. To protect the integrity and confidentiality of this data, a cryptographic model has been constructed. Fingerprints, as

a biometric characteristic, provide a high degree of specificity for the purpose of biometric identification. Tlhoolebe et al. [9] discovered a 93% classification accuracy rate for machine learning classifiers used to a private dataset of 20 persons ranging in age from 18 to 38 years in their study. The classification challenge demands the use of the KNN, Support Vector Machine (SVM), Kstar, and NB [10] algorithms. A dataset of 400 trials was used to evaluate the suggested approach. The acquired statistics show a 37% false rejection rate and a 27% false acceptance rate. The results shown are quite promising and point to the efficacy of the proposed approach. The findings suggest that the method's efficacy could be improved by combining it with another biometric. Gender classification is one of the fields of biometric authentication. FaceNet feature extraction algorithm was developed by Adhinata et al. [11]. For analyzing the IMDB dataset, the researchers used the KNN, SVM, and DT [12] algorithms. Their research revealed that the KNN method had the highest level of accuracy, with a 95.75% accuracy rate. A database containing a large number of 3408 fingerprint images. Kruti et al. [13] used an SVM classifier on a private dataset to achieve an elevated level of accuracy, reaching 97% in their study. Nguyen et al. [14] attempted to reduce the number of comparisons in automatic fingerprint recognition systems while dealing with large databases in their study. The researchers used a variety of techniques to accomplish this, including RF [15], SVM, Convolutional Neural Network (CNN), and KNN. The FVC 2000, 2002, and 2004 datasets were used to test these techniques. The algorithms were evaluated by analyzing precision, recall, accuracy, and receiver operating characteristic analysis. The results of the research showed the RF algorithm had the highest level of accuracy among the examined algorithms. The value expressed is 96.75%. The SVM method outperforms the competition, with an accuracy rate of 95.5% on two-thirds of the databases. It is proposed that supervised classification approaches such as DT, linear discriminant analysis, medium Gaussian SVM, KNN, and bagged tree ensemble classifiers should be employed to improve the efficiency of fingerprint identification systems.

The authors, Noor et al. [16], applied a methodology that included image enhancement, binarization, and preprocessing techniques in fingerprint analysis. They utilized medium Gaussian SVM classifiers to achieve an impressive accuracy rate of 98.90%. Kumar et al. [17] presented the gravitational search decision forest technique for fingerprint recognition in their research. The suggested approach combines the gravitational search algorithm and the RF method. To discover a suitable solution, the DT method was used to evaluate multiple hypotheses. The method was tested using the NIST SD27 and FVC2004 datasets. The proposal had a 92.56% average recognition rate for the NIST SD27 dataset and a 96.56% recognition rate for the FVC2004 dataset. Table 1 focuses on some of the work achieved so far to recognize fingerprints or classify fingerprints.

Table 1. Related work

Authour(s)	**Method**	**Dataset**	**Score (%)**
Labati et al. [18]	CNN	DB Latent database	89.6
	$CNN+ KNN$		46.4
	$CNN+NB$		52.1
	$CNN+SVM$		49.2
Kumar et al. [17]	RF	NIST SD27	92.56
		FVC2004	96.56
Tlhoolebe et al. [9]	KNN, SVM	Private data	93
Jang et al. [19]	DeepPore	High-Resolution-Fingerprint database	93.09
Nguyen et al. [14]	SVM	FVC2000, FVC2002, FVC2004	95.5
Adhinata et al. [11]	KNN	IMDB dataset	95.75
Heidari et al. [7]	Entropy-based pattern	Poly-U finger knuckle print	98.5
Jeon et al. [20]	VGGNet	FVC2000, FVC2002, FVC2004	82.1
	GNet		94.2
	VGGNet + Ensemble		98.3
Saeed et al. [21]	DeepFKTNet Model	FingerPass, FVC2004	98.89
Nahar et al. [22]	Self-Regulating CNN	FVC2004	99.1
Walhazi et al. [23]	Multi-Classifier System	NIST SD27, NIST SD301, FVC2002	100

3. **Methods**

3.1. *Preliminaries*

Definition 3.1. Let $f(x,y) = \mathcal{I}(i,j)_{m\times n} \in \mathbb{R}^2$ be an image, then the zero padding for neutrosophic image P_{k_0} is defined with respect to h as follows: [24]

$$P_{k_0}(g(x,y)) = \begin{cases} f(x,y) & \text{if } x+h, y+h \leq \max m, \max n \text{ or} \\ & x-h, y-h < \min m, \min n \\ 0 & \text{if } x-h, y-h \geq \min m, \min n \text{ or} \\ & x+h, y+h > \max m, \max n \end{cases} \tag{1}$$

where $k = 2\mathbb{N}+1$, $3 \leq k \leq \min(m,n)$ and $h = k \mod (2)$.

Definition 3.2. Let $f(x,y) = \mathcal{I}(i,j)_{m\times n}$ be an image then the set of arithmetic mean μ values for h of the image is defined as [24]

$$g_\mu(x,y) = \{f_1\mu_1, f_2\mu_2, ...f_c\mu_c\} \tag{2}$$

$$f_c\mu_c = \frac{1}{h^2}\sum_{k=i-\Delta i}^{i+\Delta i}\sum_{l=j-\Delta i}^{j+\Delta i} f_c(k,l) \tag{3}$$

where $c = \{1, 2, ... \min(m, n)\}$ and $\Delta i, \Delta j = \{1, 2, .. \leq h\}$

Definition 3.3. Let $f(x, y) = \mathcal{I}(i, j)_{m\times n}$ be an image then the set of standard deviation σ values for h of the image is defined as [24]

$$\begin{aligned} g_\sigma(x, y) &= \{f_1\sigma_1, f_2\sigma_2, ...f_c\sigma_c\} \\ f_c\sigma_c &= \sqrt{\frac{1}{h^2}\sum_{k=i-\Delta i}^{i+\Delta i}\sum_{l=j-\Delta j}^{j+\Delta j}(f_c(k, l) - f_c\mu_c)^2} \end{aligned} \tag{4}$$

where $c = \{1, 2, ... \min(m, n)\}$ and $\Delta i, \Delta j = \{1, 2, .. \leq h\}$

Definition 3.4. Let $f(x, y) = \mathcal{I}(i, j)_{m\times n}$ be an image then the set of maximum λ values for h of the image is defined as

$$\begin{aligned} g_\lambda(x, y) &= \{f_1\lambda_1, f_2\lambda_2, ...f_c\lambda_c\} \\ f_c\lambda_c &= \max(f_c(i \pm \Delta i, j \pm \Delta j)) \end{aligned} \tag{5}$$

where $c = \{1, 2, ... \min(m, n)\}$ and $\Delta i, \Delta j = \{1, 2, .. \leq h\}$

3.2. *Proposed Method*

The proposed method involves the utilization of a hypotheses function $H(N_A)$ to determine the values of the neutrosophic membership components. The hypothesis function for the neutrosophic components may vary depending on the approach chosen.

Definition 3.5 $(MBNI_B)$**.** Let $A = \mathcal{I}(i, j)_{m\times n}$ be an image then the neutrosophic components of A is defined as $N_A = \{T_A(i, j), I_A(i, j), F_A(i, j)\}$. The Membership Based Neutrosophic Binary Image $(MBNI_B)$ is formulated as follows:

$$\begin{aligned} \mathcal{NI}_\mathcal{B}(A) &= f(A, P_{k_0}, N_A, H(N_A)) \\ \text{where } f(A) &= \mathcal{I}(i, j)_{m\times n} \\ f(P_{k_0}) &= P_{k_0}(A(i, j)) \\ f(N_A) &= \{f(P_{k_0}(T_A)), f(P_{k_0}(I_A)), f(P_{k_0}(F_A))\} \\ f(H(N_A)) &= \{H_1(N_A), H_2(N_A), H_3(N_A), H_4(N_A)\} \end{aligned}$$

$H(N_A)$ refers the four types of hypothesis for the neutrosophic membership functions $f(N_A)$

$H_1(N_{A(i,j)})$**:** $f(P_{k_0}(T_{A(i,j)})) > \max[f(P_{k_0}(I_{A(i,j)})), f(P_{k_0}(F_{A(i,j)}))]$

$H_2(N_{A(i,j)})$**:** $f(P_{k_0}(I_{A(i,j)})) > \max[f(P_{k_0}(T_{A(i,j)})), f(P_{k_0}(F_{A(i,j)}))]$ and
$d_1(I_A) > d_2(I_A)$ where
$d_1(I_A) = f(P_{k_0}(I_{A(i,j)})) - f(P_{k_0}(T_{A(i,j)}))$
$d_2(I_A) = f(P_{k_0}(I_{A(i,j)})) - f(P_{k_0}(F_{A(i,j)}))$

$H_3(N_{A(i,j)})$: $f(P_{k_0}(I_{A(i,j)})) > \max[f(P_{k_0}(T_{A(i,j)})), f(P_{k_0}(F_{A(i,j)}))]$ and
$d_1(I_A) < d_2(I_A)$ where
$d_1(I_A) = f(P_{k_0}(I_{A(i,j)})) - f(P_{k_0}(T_{A(i,j)}))$
$d_2(I_A) = f(P_{k_0}(I_{A(i,j)})) - f(P_{k_0}(F_{A(i,j)}))$

$H_4(N_{A(i,j)})$: $f(P_{k_0}(F_{A(i,j)})) > \max[f(P_{k_0}(T_{A(i,j)})), f(P_{k_0}(I_{A(i,j)}))]$

$$\mathcal{NI}_{\mathcal{B}}(A) = \begin{cases} \mathcal{L}-1 & \text{if } H_1(N_{A(i,j)}) \text{ or } H_2(N_{A(i,j)}) \\ 0 & \text{if } H_3(N_{A(i,j)}) \text{ or } H_4(N_{A(i,j)}) \end{cases} \tag{6}$$

Definition 3.6 ($MBNI_{SI}$)**.** Let $A = \mathcal{I}(i,j)_{m\times n}$ be an image then the neutrosophic components of A is defined as $N_A = \{T_A(i,j), I_A(i,j), F_A(i,j)\}$. The Membership Based Neutrosophic Self Intensity Image ($MBNI_{SI}$) is formulated as follows

$$\begin{aligned} \mathcal{NI}_{\mathcal{SI}}(A) &= f(A, P_{k_0}, N_A, H(N_A), \xi(N_A)) \\ \text{where } f(A) &= \mathcal{I}(i,j)_{m\times n} \\ f(P_{k_0}) &= P_{k_0}(A(i,j)) \\ f(N_A) &= \{f(P_{k_0}(T_A)), f(P_{k_0}(I_A)), f(P_{k_0}(F_A))\} \\ f(H(N_A)) &= \{H_1(N_A), H_2(N_A), H_3(N_A), H_4(N_A)\} \\ f(\xi(N_A)) &= \{f_\mu(A), f_\sigma(A), f_\lambda(A)\} \end{aligned}$$

$H(N_A)$ refers the four types of hypothesis for the neutrosophic membership functions $f(N_A)$

$H_1(N_{A(i,j)})$: $f(P_{k_0}(T_{A(i,j)})) > \max[f(P_{k_0}(I_{A(i,j)})), f(P_{k_0}(F_{A(i,j)}))]$

$H_2(N_{A(i,j)})$: $f(P_{k_0}(I_{A(i,j)})) > \max[f(P_{k_0}(T_{A(i,j)})), f(P_{k_0}(F_{A(i,j)}))]$ and
$d_1(I_A) > d_2(I_A)$ where
$d_1(I_A) = f(P_{k_0}(I_{A(i,j)})) - f(P_{k_0}(T_{A(i,j)}))$
$d_2(I_A) = f(P_{k_0}(I_{A(i,j)})) - f(P_{k_0}(F_{A(i,j)}))$

$H_3(N_{A(i,j)})$: $f(P_{k_0}(I_{A(i,j)})) > \max[f(P_{k_0}(T_{A(i,j)})), f(P_{k_0}(F_{A(i,j)}))]$ and
$d_1(I_A) < d_2(I_A)$ where
$d_1(I_A) = f(P_{k_0}(I_{A(i,j)})) - f(P_{k_0}(T_{A(i,j)}))$
$d_2(I_A) = f(P_{k_0}(I_{A(i,j)})) - f(P_{k_0}(F_{A(i,j)}))$

$H_4(N_{A(i,j)})$: $f(P_{k_0}(F_{A(i,j)})) > \max[f(P_{k_0}(T_{A(i,j)})), f(P_{k_0}(I_{A(i,j)}))]$

$$\mathcal{NI}_{\mathcal{SI}}(A) = \begin{cases} f(A(i,j)) & \text{if } H_1(N_{A(i,j)}) \\ f_\mu(A(i,j)) & \text{if } H_2(N_{A(i,j)}) \\ \mid f_\mu(A(i,j)) - f_\sigma(A(i,j)) \mid \in \mathbb{Z}^+ & \text{if } H_3(N_{A(i,j)}) \\ 0 & \text{if } H_4(N_{A(i,j)}) \text{ or otherwise} \end{cases} \tag{7}$$

Definition 3.7 ($MBSVNI_B$)**.** Let $A = \mathcal{I}(i,j)_{m\times n}$ be an image then the neutrosophic components of A is defined as $SVN_A = \{T_A(i,j), I_A(i,j), F_A(i,j)\}$. The Membership Based Single

Valued Neutrosophic Binary Image ($MBSVNI_B$) is formulated as follows

$$\begin{aligned}
\mathcal{SVNI}_{\mathcal{B}}(A) &= f(A, P_{k_0}, SVN_A, H(SVN_A)) \\
\text{where } f(A) &= \mathcal{I}(i,j)_{m\times n} \\
f(P_{k_0}) &= P_{k_0}(A(i,j)) \\
f(SVN_A) &= \{f(P_{k_0}(T_A)), f(P_{k_0}(I_A)), f(P_{k_0}(F_A))\} \\
f(H(SVN_A)) &= \{H_1(SVN_A), H_2(SVN_A), H_3(SVN_A), H_4(SVN_A)\}
\end{aligned}$$

$H(SVN_A)$ refers the four types of hypothesis for the neutrosophic membership functions $f(SVN_A)$

$H_1(SVN_{A(i,j)})$**:** $f(P_{k_0}(T_{A(i,j)})) > \max[f(P_{k_0}(I_{A(i,j)})), f(P_{k_0}(F_{A(i,j)}))]$

$H_2(SVN_{A(i,j)})$**:** $f(P_{k_0}(I_{A(i,j)})) > \max[f(P_{k_0}(T_{A(i,j)})), f(P_{k_0}(F_{A(i,j)}))]$ and

$d_1(I_A) > d_2(I_A)$ where

$d_1(I_A) = f(P_{k_0}(I_{A(i,j)})) - f(P_{k_0}(T_{A(i,j)}))$

$d_2(I_A) = f(P_{k_0}(I_{A(i,j)})) - f(P_{k_0}(F_{A(i,j)}))$

$H_3(SVN_{A(i,j)})$**:** $f(P_{k_0}(I_{A(i,j)})) > \max[f(P_{k_0}(T_{A(i,j)})), f(P_{k_0}(F_{A(i,j)}))]$ and

$d_1(I_A) < d_2(I_A)$ where

$d_1(I_A) = f(P_{k_0}(I_{A(i,j)})) - f(P_{k_0}(T_{A(i,j)}))$

$d_2(I_A) = f(P_{k_0}(I_{A(i,j)})) - f(P_{k_0}(F_{A(i,j)}))$

$H_4(SVN_{A(i,j)})$**:** $f(P_{k_0}(F_{A(i,j)})) > \max[f(P_{k_0}(T_{A(i,j)})), f(P_{k_0}(I_{A(i,j)}))]$

$$\mathcal{SVNI}_{\mathcal{B}}(A) = \begin{cases} \mathcal{L}-1 & \text{if } H_1(SVN_{A(i,j)}) \text{ or } H_2(SVN_{A(i,j)}) \\ 0 & \text{if } H_3(SVN_{A(i,j)}) \text{ or } H_4(SVN_{A(i,j)}) \end{cases} \tag{8}$$

Definition 3.8 ($MBSVNI_{SI}$)**.** Let $A = \mathcal{I}(i,j)_{m\times n}$ be an image then the neutrosophic components of A is defined as $SVN_A = \{T_A(i,j), I_A(i,j), F_A(i,j)\}$. The Membership Based Single Valued Neutrosophic Self Intensity Image ($MBSVNI_{SI}$) is formulated as follows

$$\begin{aligned}
\mathcal{SVNI}_{\mathcal{SI}}(A) &= f(A, P_{k_0}, SVN_A, H(SVN_A), \xi(SVN_A)) \\
\text{where } f(A) &= \mathcal{I}(i,j)_{m\times n} \\
f(P_{k_0}) &= P_{k_0}(A(i,j)) \\
f(SVN_A) &= \{f(P_{k_0}(T_A)), f(P_{k_0}(I_A)), f(P_{k_0}(F_A))\} \\
f(H(SVN_A)) &= \{H_1(SVN_A), H_2(SVN_A), H_3(SVN_A), H_4(SVN_A)\} \\
f(\xi(SVN_A)) &= \{f_\mu(A), f_\sigma(A), f_\lambda(A)\}
\end{aligned}$$

$H(SVN_A)$ refers the four types of hypothesis for the neutrosophic membership functions $f(SVN_A)$

$H_1(SVN_{A(i,j)})$**:** $f(P_{k_0}(T_{A(i,j)})) > \max[f(P_{k_0}(I_{A(i,j)})), f(P_{k_0}(F_{A(i,j)}))]$

$H_2(SVN_{A(i,j)})$: $f(P_{k_0}(I_{A(i,j)})) > \max[f(P_{k_0}(T_{A(i,j)})), f(P_{k_0}(F_{A(i,j)}))]$ and
$d_1(I_A) > d_2(I_A)$ where
$d_1(I_A) = f(P_{k_0}(I_{A(i,j)})) - f(P_{k_0}(T_{A(i,j)}))$
$d_2(I_A) = f(P_{k_0}(I_{A(i,j)})) - f(P_{k_0}(F_{A(i,j)}))$
$H_3(SVN_{A(i,j)})$: $f(P_{k_0}(I_{A(i,j)})) > \max[f(P_{k_0}(T_{A(i,j)})), f(P_{k_0}(F_{A(i,j)}))]$ and
$d_1(I_A) < d_2(I_A)$ where
$d_1(I_A) = f(P_{k_0}(I_{A(i,j)})) - f(P_{k_0}(T_{A(i,j)}))$
$d_2(I_A) = f(P_{k_0}(I_{A(i,j)})) - f(P_{k_0}(F_{A(i,j)}))$
$H_4(SVN_{A(i,j)})$: $f(P_{k_0}(F_{A(i,j)})) > \max[f(P_{k_0}(T_{A(i,j)})), f(P_{k_0}(I_{A(i,j)}))]$

$$\mathcal{SVNI}_{\mathcal{SI}}(A) = \begin{cases} f(A(i,j)) & \text{if } H_1(SVN_{A(i,j)}) \\ f_\mu(A(i,j)) & \text{if } H_2(SVN_{A(i,j)}) \\ \mid f_\mu(A(i,j)) - f_\sigma(A(i,j)) \mid \in \mathbb{Z}^+ & \text{if } H_3(SVN_{A(i,j)}) \\ 0 & \text{if } H_4(SVN_{A(i,j)}) \text{ or otherwise} \end{cases} \tag{9}$$

FIGURE 1. Fingerprint image visualization of proposed methods

From the Figure 1 proposal can visualize the patterns of proposed methods fingerprint image.

3.3. *Auto Hyper parameterization*

Definition 3.9. Consider $N\mathcal{I}_A$ be a neutrosophic binary image of the image A then the Bernoulli distribution values for h convolution is calculated as follows:

Let $B(i,j,h)_c = \{N\mathcal{I}_{A(i\pm\Delta i, j\pm\Delta j)^1}, N\mathcal{I}_{A(i\pm\Delta i, j\pm\Delta j)^2}, \cdots N\mathcal{I}_{A(i\pm\Delta i, j\pm\Delta j)^c}\}$ the quantity of successive events $\mathcal{L}-1$ for h and their probability $\bar{\mu}$ are

$$\begin{aligned} \mathcal{B}(N\mathcal{I}_A, e_1^\nu, \bar{\mu}_1^\nu) &= \binom{c}{e_1^\nu} (\bar{\mu}_1^\nu)^{e_1^\nu} (1-\bar{\mu}_1^\nu)^{c-e_1^\nu} \\ \text{where } e_1^\nu &= e_1^\nu(B(i,j,h)_c) = \{n_{\mathcal{L}-1}(e_1), n_{\mathcal{L}-1}(e_2), \cdots n_{\mathcal{L}-1}(e_\nu)\} \\ \bar{\mu}_1^\nu &= \bar{\mu}_1^\nu(B(i,j,h)_c) = \bar{\mu}(B(i,j,h)_1^\nu) \end{aligned} \tag{10}$$

Definition 3.10. Consider $N\mathcal{I}_A$ be a neutrosophic self intensity image of the image A then the Gaussion distribution values for h convolution is calculated as follows:
Let $B(i,j,h)_c = \{N\mathcal{I}_{A(i\pm\Delta i,j\pm\Delta j)^1}, N\mathcal{I}_{A(i\pm\Delta i,j\pm\Delta j)^2}, \cdots N\mathcal{I}_{A(i\pm\Delta i,j\pm\Delta j)^c}\}$ then the mean $\bar{\mu}$ and standard deviation $\bar{\sigma}$ values for h

$$\begin{aligned} \mathcal{G}(N\mathcal{I}_A, \bar{\mu}_{c_1^\nu}, \bar{\sigma}_{c_1^\nu}) &= \frac{1}{\bar{\sigma}_{c_1^\nu}\sqrt{2\pi}} e^{-\frac{1}{2}\left(\frac{N\mathcal{I}_{A(i,j)} - \bar{\mu}_{c_1^\nu}}{\bar{\sigma}_{c_1^\nu}}\right)^2} \\ \bar{\mu}_{c_1^\nu} &= \bar{\mu}(B(i,j,h)_{c_1^\nu}) \\ \bar{\sigma}_{c_1^\nu} &= \bar{\sigma}(B(i,j,h)_{c_1^\nu}) \end{aligned} \tag{11}$$

Definition 3.11. For the neutrosophic image $N\mathcal{I}_A$ generalized parameters are formulated as follows

$$\Theta_A = \{\theta_1, \theta_2, ...\theta_t\} \tag{12}$$

$$\text{where } \theta_t = \begin{cases} \mathcal{B}(N\mathcal{I}_A, e_1^\nu, \bar{\mu}_1^\nu) & \text{if } N\mathcal{I}_A \text{ is binary image} \\ \mathcal{G}(N\mathcal{I}_A, \bar{\mu}_{c_1^\nu}, \bar{\sigma}_{c_1^\nu}) & \text{if } N\mathcal{I}_A \text{ is self intensity image} \end{cases}$$

$$\xi_A = \{\xi_1, \xi_2, ...\xi_t\} \tag{13}$$

$$\text{where } \xi_t = \bar{\bar{\theta}}_t$$

3.4. *Parameter tuning*

For instance analysis, article suggest default classification data, digits data from the Sklearn dataset [25].

3.4.1. *Decision tree classifier*

DT possesses multiple properties that can be tweaked to improve performance. Maximum depth, minimum sample split, minimum sample leaf, and minimum weighted fraction are among these parameters. This proposal takes into account the first three criteria for classification. The attribute "maximum depth" is in charge of determining the tree's maximum depth. "Tree height" refers to the maximum length of a path from a tree's root to any of its leaves. The minimum split refers to the minimum number of values that must be present in a node before attempting a split operation. To clarify, if a node has only two members and the minimum split criterion is set to 5, the node will enter a terminal state, preventing any further efforts to split it. The minimal sample split denotes the smallest number of entities that can exist in a tree's leaf node. The default value is one-third of the minimum split value

Algorithm 1 Proposed method and hyperparameters tuning algorithm

Require: Input Image database, classification labels

```
for i in image do
    MBNI_B, MBNI_SI
    MBSVNI_B, MBSVNI_SI
    if i is MBNI_B or MBSVNI_B then
        B(NI_A, e_1^ν, μ̄_1^ν) ← Equation 10
    else if i is MBNI_SI or MBSVNI_SI then
        G(NI_A, μ̄_{c_1^ν}, σ̄_{c_1^ν}) ← Equation 11
    end if
    parameters = {Θ_A, ξ_A}
end for
if model = DT then ← Equation 14
    for i = ξ_A do
        h_{p(md)}
        for j= ξ_A do
            h_{p(msl)}
            for k = Θ_A do
                h_{p(mss)}
                model.fit(parameters = i, j, k)
            end for
        end for
    end for
end if
if model = RF then ← Equation 15
    for i = ξ_A do
        h_{p(mss)}
        for j = ξ_A do
            h_{p(msl)}
            for k = Θ_A do
                h_{p(mw)}
                model.fit(parameters = i, j, k)
            end for
        end for
    end for
end if
```

if model = LR **then** ← Equation 16
  for i = Θ_A **do**
    $h_{p(tol)}$
    model.fit(parameters = i)
  end for
end if
if model = NB **then** ← Equation 17
  for i = Θ_A **do**
    $h_{p(nb)}$
    for j =Θ_A **do**
      $h_{p(bin)}$
      model.fit(parameters = i, j)
    end for
  end for
end if
if model = KNN **then** ← Equation 18
  for i = Θ_A **do**
    $h_{p(nb)}$
    for j = Θ_A **do**
      $h_{p(ls)}$
      for k = Θ_A **do**
        $h_{p(p)}$
        model.fit(parameters = i, j, k)
      end for
    end for
  end for
end if

specified. The following is the formulation of attribute value selection:

$$\begin{aligned} DT &= f(X, Y, h_p) \\ \text{where } f(h_p) &= \{h_{p(md)}, h_{p(mss)}, h_{p(msl)}\} \\ h_{p(md)} &= \xi_A(2 \times \sqrt{\min(m, n)}) \\ h_{p(mss)} &= \lfloor | \log_e \Theta_A | \rfloor = \lfloor | \log_e \theta_t | \rfloor \\ h_{p(msl)} &= \xi_A \mod (2h) \end{aligned} \tag{14}$$

The utilization of least cost-complexity pruning technique is aimed at mitigating the issue of over fitting in decision tree classification. In the context of cost-complexity pruning, the process is carried out recursively to identify the node that exhibits the lowest level of strength

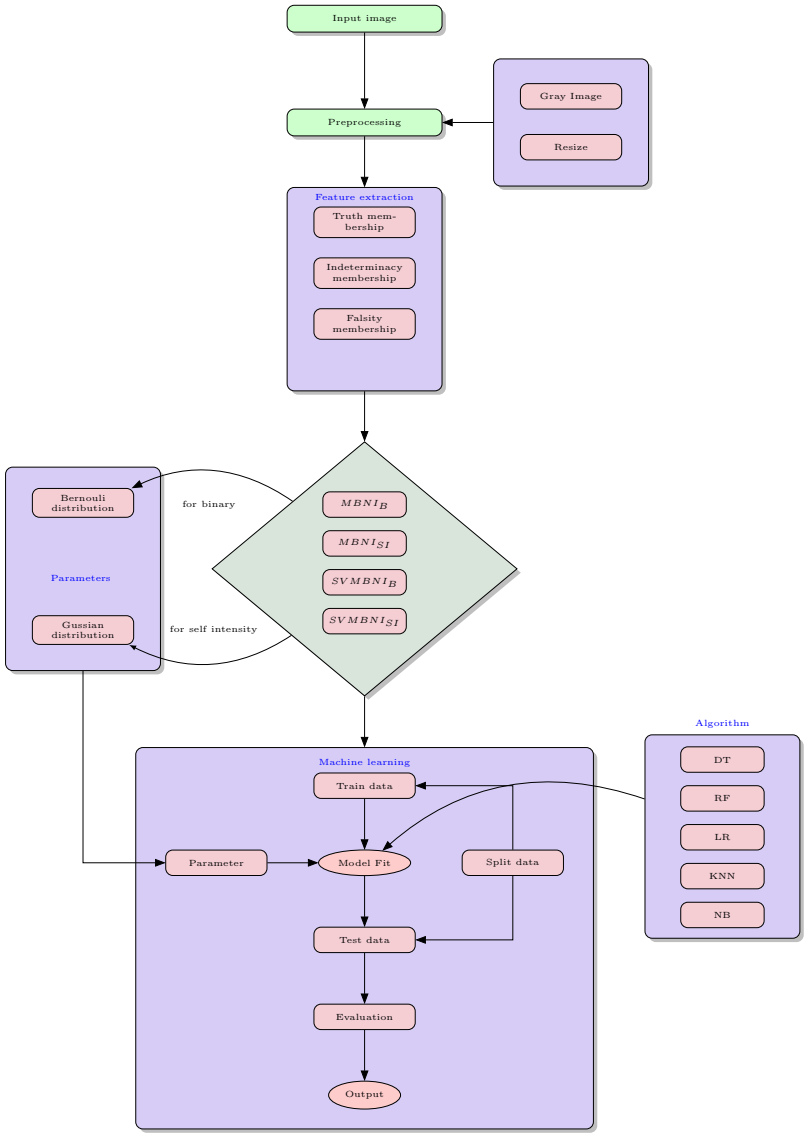

FIGURE 2. Procedure flow chart of the proposed model

or effectiveness. The implementation of an efficient α, which prioritizes the pruning of nodes associated with the intuitive reader interface α, facilitates the identification of the most vulnerable component. The determination of ideal α values in the pruning process involves assessing the effectiveness of α and the corresponding total leaf impurity at each stage. As the value of α increases, a greater portion of the tree will require pruning, resulting in an elevation of the overall impurity of the leaves. The aforementioned equation yields α values of 2 and 4 for the dataset. The association between leaf impurity and α effectiveness for each α value in the training and testing data is shown in Figure 3.

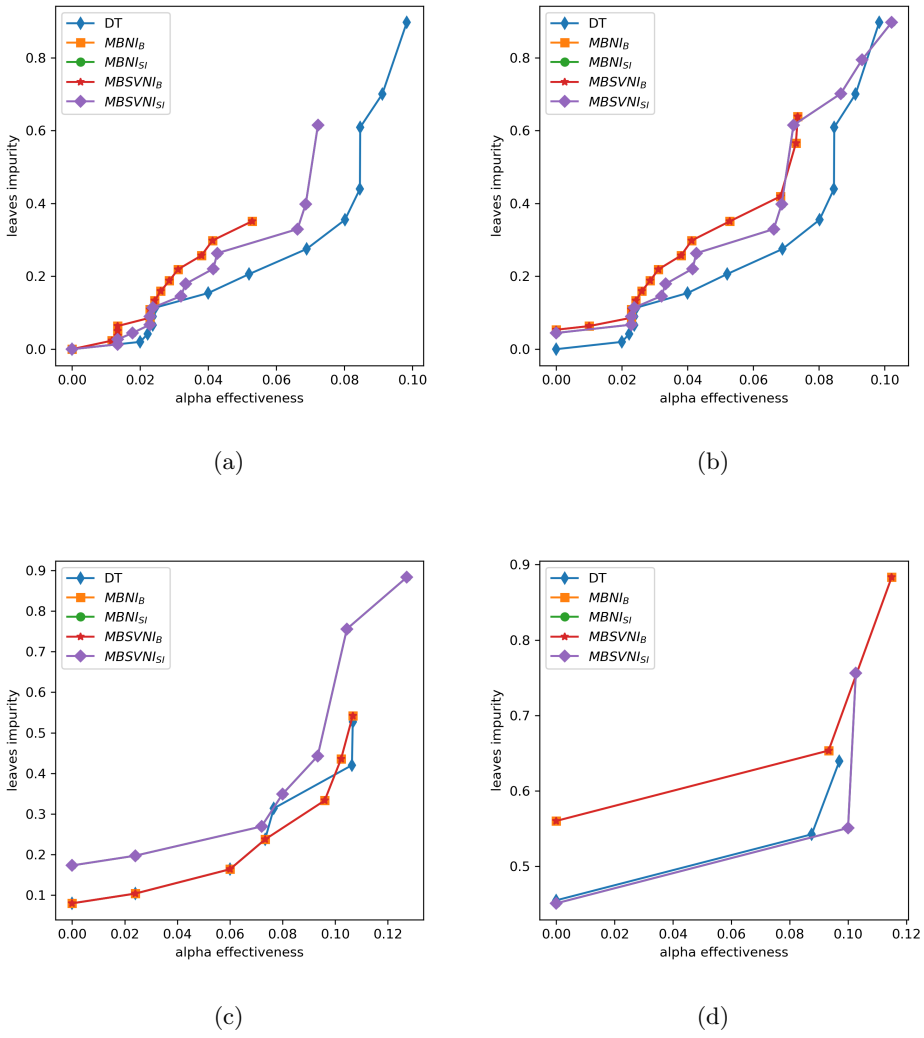

FIGURE 3. Total Impurity vs effective α for training and testing data (a) $\alpha = 2$ training data (b) $\alpha = 4$ training data (c) $\alpha = 2$ testing data (d) $\alpha = 4$ testing data

3.4.2. *Random forest*

The proposal addresses the *RF* algorithm's three hyperparameters: minimum sample split, minimum sample leaf, and minimum weight fraction leaf. *DT* previously covered the minimum sample split and minimum sample leaf. This algorithm will also go through the smallest weighted fraction attribute. This attribute represents the total of the weights required to be at a leaf node. It is comparable to the minimal sample size but uses a fraction of the total number of observations instead. However, the approach of *RF* attribute formulation varies

from that of the DT. The RF algorithm's attribute formulation is calculated below.

$$\begin{aligned} RF &= f(X, Y, h_p) \\ \text{where } f(h_p) &= \{h_{p(md)}, h_{p(mss)}, h_{p(msl)}\} \\ h_{p(mss)} &= \xi_A \mod (\sqrt{\min(m,n)}) > 0 \\ h_{p(msl)} &= \xi_A \mod (\sqrt{\min(m,n)}) > 1 \\ h_{p(mw)} &= -\log_2 \Theta_A \times 10^3 \end{aligned} \tag{15}$$

To test the relevance of features, evaluate the mean drop in accuracy of the forest when the features are randomly permuted in out-of-bag samples. This measurement is also known as permutation importance since it shows the former is experimentally biased towards unique predictor variables. This bias stems from an unfair advantage granted by the standard impurity functions to predictors with a large number of values in the case of a single DT. The mean loss in accuracy is significantly biased in this case to exaggerate the impact of associated variables. The comparison plot in Figure 4 revealed the mean decreased accuracy for the consideration data for the traditional RF method and the novel RF method.

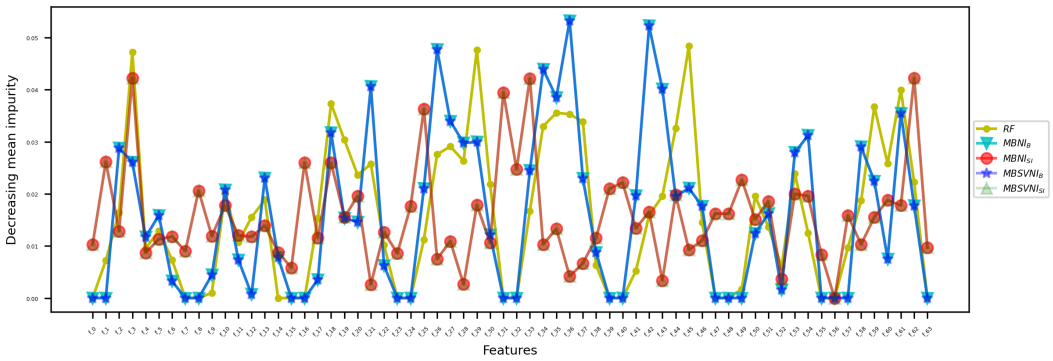

FIGURE 4. Comparison analysis of random forest feature importance

3.4.3. *Logistic regression*

We modify a parameter called tolerance in LR [26]. The size of a tolerance interval is proportional to the size of the population data sample and the population variation. Depending on the data distribution, there are two primary methods for computing tolerance intervals: parametric and non parametric methods. Interval of metric tolerance: To describe coverage and confidence, use knowledge of the population distribution, which is used to refer to a Gaussian distribution. Non parametric tolerance interval: Estimate coverage and confidence using rank statistics, which sometimes results in less precision due to a lack of knowledge about the distribution. The comparison with the pixel relation is accomplished here by varying the

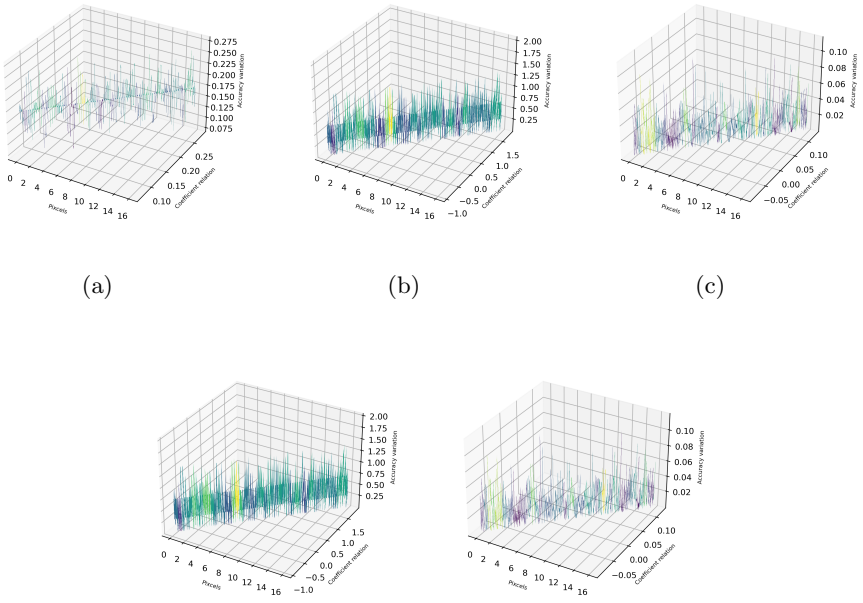

(a) (b) (c)

(d) (e)

FIGURE 5. Logistic regression analysis (a) Classic method, (b)$MBNI_B$-method, (c) $MBNI_{SI}$-method, (d) $MBSVNI_B$-method, (e) $MBSVNI_{SI}$-method

accuracy of the pixel's correlation coefficients. The relational analysis of the LR technique and NS-based LR approaches is depicted in Figure 5.

$$\begin{aligned} LR &= f(X, Y, h_p) \\ \text{where } f(h_p) &= \{h_{p(tol)}\} \\ h_{p(tol)} &= (-\log_2 \Theta_A) \times 10^3 \end{aligned} \tag{16}$$

3.4.4. *Naive Bayes*

For data with multivariate Bernoulli distributions, Bernoulli NB applies the NB training and classification algorithms. This indicates that several features may exist, but each appears to be a binary-valued variable. The NB method has only two basic parameters: α and

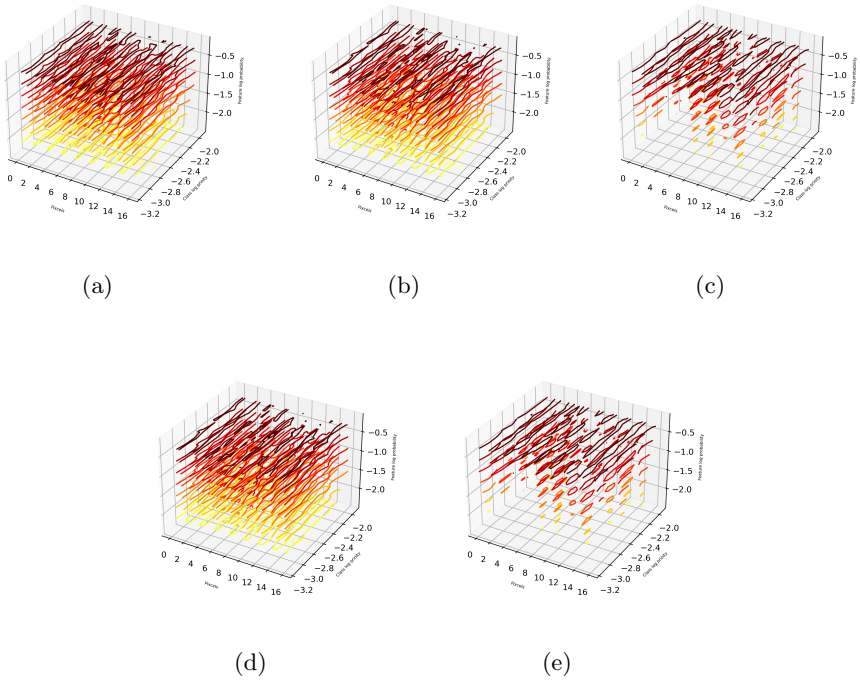

(a) (b) (c)

(d) (e)

FIGURE 6. Naive Bayes analysis (a) Classic method, (b)$MBNI_B$-method, (c) $MBNI_{SI}$-method, (d) $MBSVNI_B$-method, (e) $MBSVNI_{SI}$-method

binarization values.

$$\begin{aligned} NB &= f(X, Y, h_p) \\ \text{where } f(h_p) &= \{h_{p(\alpha)}, h_{p(bin)}\} \\ h_{p(\alpha)} &= \mid (\log_{10} \Theta_A \times 10^{-4}) \min(m, n) \mid \\ h_{p(bin)} &= -\log_2 \Theta_A \times 10^{-3} \end{aligned} \tag{17}$$

α is the Laplace smoothing technique used in NB to solve the problem of zero probability with the prior probability and conditional probability. The estimator for a collection of observation counts $X = \{x_1, x_2, ..x_n\}$ from a n-dimensional multinomial distribution with N trials is a smoothed version of the counts as follows:

$$\theta_i = \frac{x_i + \alpha}{N + \alpha n} \quad (i = 1, 2, ..n)$$

Using these attributes, the proposal extracts image properties such as class log priority and feature log likelihood. Figure 6 demonstrates the performance of the analysis with the intensity and the extracted features. Because the feature's probability is more feasible than other ways, the proposed binary method surpasses the classical and self-intensity methods.

3.4.5. *K nearest neighbor*

KNN requires three factors into account: the number of neighborhoods, leaf size, and power parameters. The number of neighbors refers to the number of elements that comprise the classification in a single group. The preceding method, DT, explicitly addresses leaf size. The Minkowski metric is referred to by the power parameter.

$$\begin{aligned} KNN &= f(X, Y, h_p) \\ \text{where } f(h_p) &= \{h_{p(nb)}, h_{p(ls)}, h_{p(p)}\} \\ h_{p(nb)} &= \xi_A \mod (2\sqrt{\min(m,n)}) \\ h_{p(ls)} &= \xi_A \mod (\min(m,n)) \times 2\sqrt{\min(m,n)} \\ h_{p(p)} &= \xi_A \mod (\sqrt{\min(m,n)}) \end{aligned} \tag{18}$$

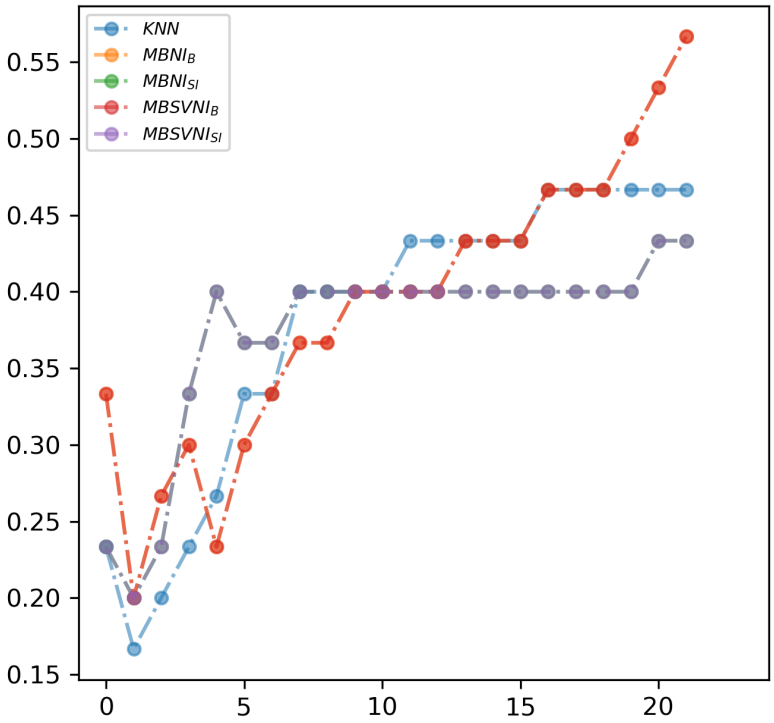

FIGURE 7. K nearest neighbourhood error analysis

The expected error of neighbourhood component analysis can be expressed as

$$err = 1 - \frac{1}{N} \sum_{i,j=1}^{N} P_{ij} y_{ij}$$

where $y_{ij} = 1$ if $y_i = y_j$ otherwise $y_{ij} = 0$. Figure 7 shows the error comparison analysis of classic KNN method and proposed KNN methods for digit classification dataset. Figure 2 indicates the process manner of the proposal.

4. **Results and Discussion**

We use hardware that supports the 11th Gen Intel(R) Core(TM) i5-1135G7 @ 2.40GHz 2.42GHz with 16 GB RAM capacity for the analysis. We render the use of Python and Sklearn packages for software [25] support. This article examines the Fingerprint Verification Competition (FVC) databases from 2000 [27] , 2002 [28], and 2004 [29]. Our various databases were collected in FVC2000 using the sensors Secure Desktop Scanner (300×300), TouchChip (256×364), DF-90 (448×478), and synthetic generation based on evolution (240×320), all with 500 dpi. FVC2002 uses three different scanners and the SFinGE synthetic generator to collect fingerprints: Identix TouchView II (388×374), Biometrika FX2000 (296×560), Precise Biometrics 100 SC (300×300), and SFinGE v2.51 (288×384) with a resolution of 500 dpi.

FVC2004 includes the first 100 fingers (800 images) of DB1, DB2, DB3, and DB4. TIF image format, 256 gray-level, uncompressed image resolution (which may vary slightly depending on the database), and 500 dpi. SD 302 [30] is a collection of distributions each containing a logical subset of the images collected for the N2N Fingerprint Challenge. SD 302a for instance only contains friction ridge imagery in Portable Network Graphics (PNG) encoding generated by the Challengers. The data collection was taken from 64.7% female participants, 35.0% male participants, and 0.3% who were not interested in revealing their gender. The labels A-H correspond to the Challenger types IDEMIA, Advanced Optical Systems, Green Bit, Cornell University, Jenetric, Touchless Biometric Systems, Undisclosed, and Clarkson University. The challengers brought their fingerprint capture devices, as well as any computer hardware and software required for fingerprint capture. Challenger wrote or obtained all software used. The challengers brought their fingerprint capture devices, as well as any computer hardware and software required for fingerprint capture. The Challenger obtained all of the software used. Each Challenger was given no more than 5 minutes with a study participant, for a total of 40 minutes of Challenger collection time. Challengers were required to submit a unique image for each finger that could be used with a commercial off-the-shelf (COTS) fingerprint identification system. Challengers could capture more than one finger at a time, but all images must depict only one finger per image. The accuracy of factors is used in this article to evaluate the performance of a fingerprint classification system using machine learning methods (RF, DT, LR, NB, KNN). Table 2 depicts the formulation of metrics formulae.

In general, resize level is an application option to achieve a sustainable result. In this case, the minimum size level = 5 and the maximum size level = 25. Even resize level 64 produces

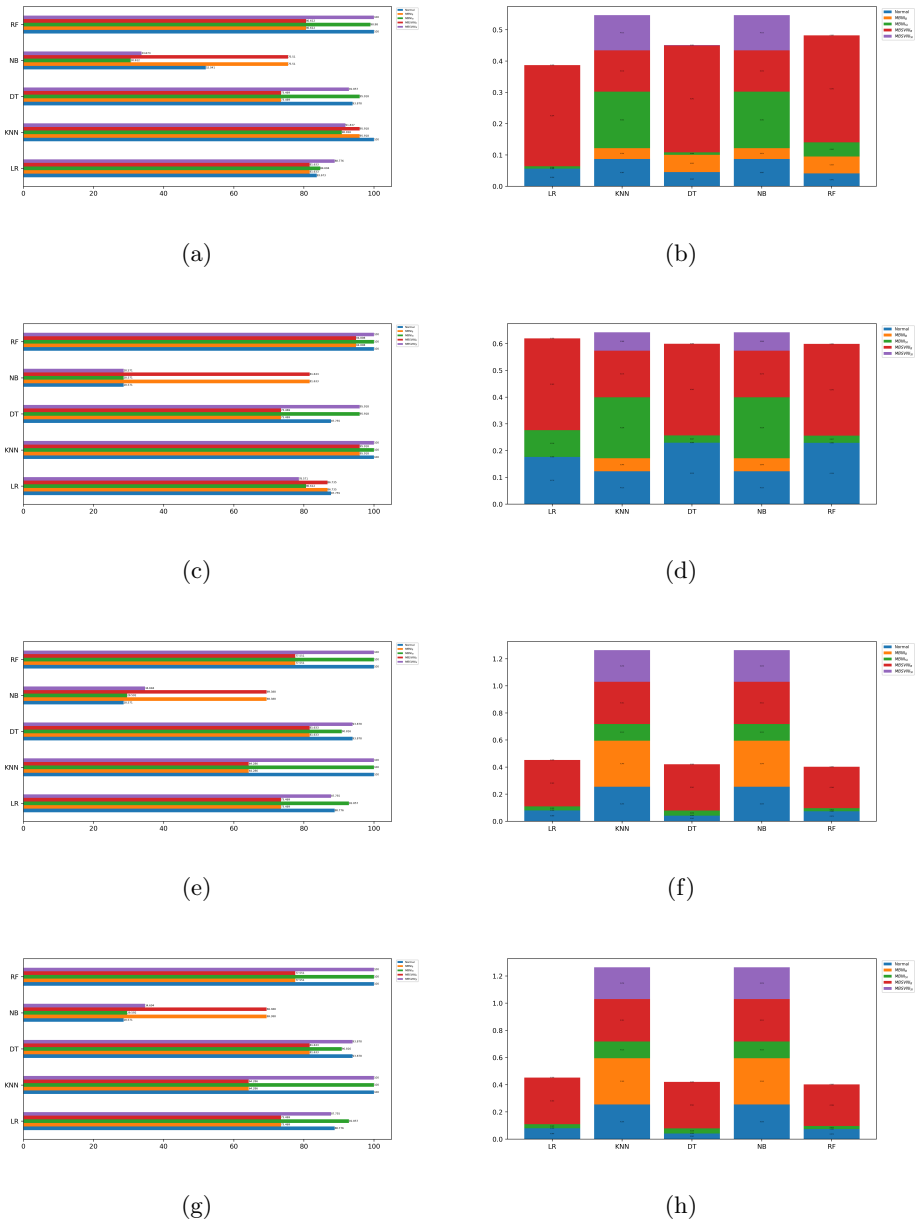

FIGURE 8. Resize level = 5, $h = 3$ comparative analysis; (a) SD302 accuracy (b) SD302 error rate (c) FVC2000 accuracy (d) FVC2000 error rate (e) FVC2002 accuracy (f) FVC2002 error rate (g) FVC2004 accuracy (h) FVC2004 error rate

the same result as size level 25. As a result, with a large size and a more reliable size of 25, the output duration is reduced resize level 64. As a result of the analysis, we chose 5 and 25 as resize factors.

Figure 8 represents the results of the classical method and the proposed neutrosophic basic methods for the obtained hyperparameters. Model selection is based on the consideration of

Table 2. Metrics

Metrics	Formula
Root mean square	$\sqrt{\sum_{i=1}^{n} \frac{(\hat{y_i}-y_i)^2}{n}}$
Precision	$\frac{True\ Positive}{True\ Positive+False\ Positive}$
Recall	$\frac{True\ Positive}{True\ Positive+False\ Negative}$
F1-score	$2.\frac{Precision.Recall}{Precision+Recall}$
Accuracy	$\frac{True\ Positive+True\ Negative}{True\ Positive+True\ Negative+False\ Positive+False\ Negative}$

a high level of accuracy while having a low number of errors. $MBNI_{SI}$ and $MBSVNI_{SI}$ perform very well in the SD302 database for the LR algorithm compared to the classical LR algorithm. $MBSVNI_{SI}$, in particular, outperforms others in terms of accuracy and error. The proposed KNN method 5% is less than the classical method for SD302 data, but when considering the error rate, the classical method is extremely large. It indicates that the reliable comfort is lower, but when considering the $MBNI_B$ error rate, it acknowledges that the accuracy level is higher than that of the classical method. The $MBNI_{SI}$ based DT method performs admirably in terms of accuracy and error values. This indicates that $MBNI_{SI}$ is considered for classification while the DT algorithm uses a smaller image size. For the NB algorithm, both the self-intensity methods $MBNI_{SI}$ and $MBSVNI_{SI}$ outperform the classical NB method, but $MBSVNI_{SI}$ has higher error values. While the comparison of these two methods, the $MBNI_{SI}$ method NB algorithm is preferable because of its high accuracy rate and low error rate, and the $MBSVNI_{SI}$ method RF algorithm performs better than other methods.

In the FVC2000 dataset, proposed self-intensity methods ($MBNI_{SI}$, $MBSVNI_{SI}$) perform very well compared to classical NB classification, and the proposed binary methods ($MBNI_B$, $MBSVNI_B$) perform very well compared to classical DT classification with a lower error rate. The proposed binary methods ($MBNI_B$,$MBSVNI_B$) perform equally well in accuracy measures for the RF and KNN algorithms. Based on their error values, the proposed binary method has a shorter error rate than the classical approach. The proposed method LR algorithm outperforms the classical LR algorithm for resizing level 5.

The FVC2002 and FVC2004 dataset performs in the same way as the FVC2000 dataset. Here also proposed $MBNI_{SI}$, $MBSVNI_{SI}$ method NB algorithm perform very well compared to classical NB classification, and the proposed binary methods $MBNI_B$, $MBSVNI_B$ perform very well compared to classical DT classification with a lower error rate and the proposed binary methods ($MBNI_B$, $MBSVNI_B$) outperform the RF and KNN algorithms in terms of accuracy and as well as error rate. The improvement over FVC2000 data is that the

TABLE 3. Result of the proposed methods

Data	Algorithm	Classic method	$\mathbf{MBNI_B}$	$\mathbf{MBNI_{SI}}$	$\mathbf{MBSVNI_B}$	$\mathbf{MBSVNI_{SI}}$
Resize = 5, h = 3						
SD302	LR	83.673±0.056	81.633±0.087	84.694±0.045	81.633±0.087	88.776±0.041
	KNN	100.0±0.0	95.918±0.034	90.816±0.055	95.918±0.034	91.837±0.054
	DT	93.878±0.008	73.469±0.181	95.918±0.008	73.469±0.181	92.857±0.045
	NB	52.041±0.324	75.51±0.132	30.612±0.341	75.51±0.132	33.673±0.342
	RF	100.0±0.0	80.612±0.112	98.98±0.002	80.612±0.112	100.0±0.0
FVC2000	LR	87.755±0.176	86.735±0.123	80.612±0.23	86.735±0.123	78.571±0.229
	KNN	100.0±0.0	95.918±0.049	100.0±0.0	95.918±0.049	100.0±0.0
	DT	87.755±0.1	73.469±0.228	95.918±0.027	73.469±0.228	95.918±0.027
	NB	28.571±0.343	81.633±0.174	28.571±0.343	81.633±0.174	28.571±0.343
	RF	100.0±0.0	94.898±0.069	100.0±0.0	94.898±0.069	100.0±0.0
FVC2002	LR	88.776±0.08	73.469±0.255	92.857±0.042	73.469±0.255	87.755±0.074
	KNN	100.0±0.0	64.286±0.34	100.0±0.0	64.286±0.34	100.0±0.0
	DT	93.878±0.029	81.633±0.123	90.816±0.038	81.633±0.123	93.878±0.023
	NB	28.571±0.343	69.388±0.311	29.592±0.341	69.388±0.311	34.694±0.306
	RF	100.0±0.0	77.551±0.234	100.0±0.0	77.551±0.234	100.0±0.0
FVC2004	LR	88.776±0.08	73.469±0.255	92.857±0.042	73.469±0.255	87.755±0.074
	KNN	100.0±0.0	64.286±0.34	100.0±0.0	64.286±0.34	100.0±0.0
	DT	93.878±0.029	81.633±0.123	90.816±0.038	81.633±0.123	93.878±0.023
	NB	28.571±0.343	69.388±0.311	29.592±0.341	69.388±0.311	34.694±0.306
	RF	100.0±0.0	77.551±0.234	100.0±0.0	77.551±0.234	100.0±0.0
Resize = 25, h=3						
SD302	LR	95.918±0.031	100.0±0.0	100.0±0.0	100.0±0.0	100.0±0.0
	KNN	100.0±0.0	100.0±0.0	100.0±0.0	100.0±0.0	100.0±0.0
	DT	92.857±0.016	90.816±0.064	90.816±0.034	90.816±0.064	90.816±0.034
	NB	53.061±0.322	96.939±0.016	42.857±0.193	96.939±0.016	50.0±0.175
	RF	100.0±0.0	100.0±0.0	100.0±0.0	100.0±0.0	100.0±0.0
FVC2000	LR	100.0±0.0	96.939±0.04	97.959±0.039	96.939±0.04	97.959±0.039
	KNN	100.0±0.0	100.0±0.0	100.0±0.0	100.0±0.0	100.0±0.0
	DT	100.0±0.0	85.714±0.121	100.0±0.0	85.714±0.121	100.0±0.0
	NB	28.571±0.343	84.694±0.154	52.041±0.283	84.694±0.154	53.061±0.281
	RF	100.0±0.0	100.0±0.0	100.0±0.0	100.0±0.0	100.0±0.0
FVC2002	LR	100.0±0.0	100.0±0.0	100.0±0.0	100.0±0.0	98.98±0.005
	KNN	100.0±0.0	100.0±0.0	100.0±0.0	100.0±0.0	100.0±0.0
	DT	98.98±0.005	76.531±0.246	94.898±0.021	76.531±0.246	94.898±0.021
	NB	35.714±0.335	89.796±0.086	65.306±0.419	89.796±0.086	87.755±0.121
	RN	100.0±0.0	100.0±0.0	100.0±0.0	100.0±0.0	100.0±0.0
FVC2004	LR	100.0±0.0	100.0±0.0	100.0±0.0	100.0±0.0	98.98±0.005
	KNN	100.0±0.0	100.0±0.0	100.0±0.0	100.0±0.0	100.0±0.0
	DT	98.98±0.005	76.531±0.246	94.898±0.021	76.531±0.246	94.898±0.021
	NB	35.714±0.335	89.796±0.086	65.306±0.419	89.796±0.086	87.755±0.121
	RF	100.0±0.0	100.0±0.0	100.0±0.0	100.0±0.0	100.0±0.0

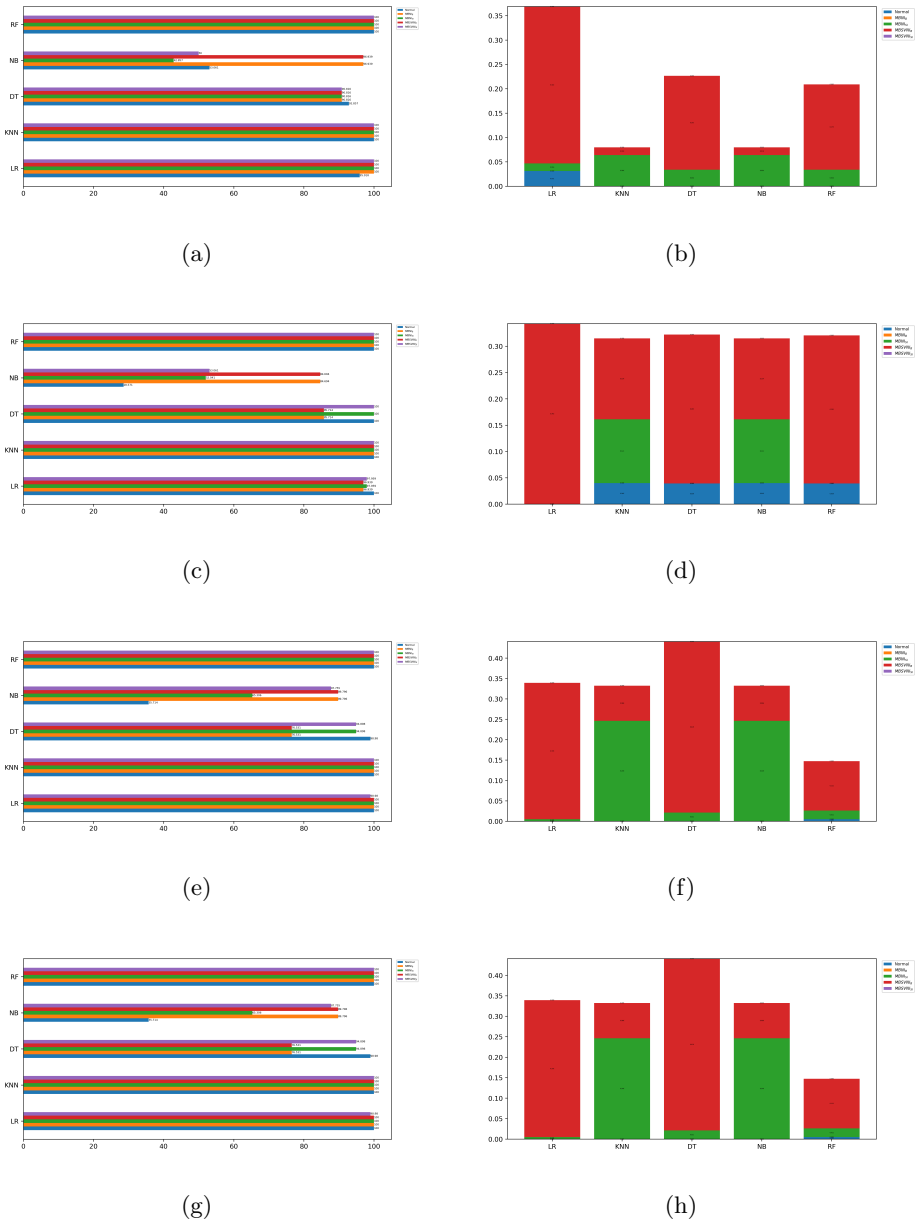

FIGURE 9. Resize level = 25, $h = 3$ comparative analysis; (a) SD302 accuracy (b) SD302 error rate (c) FVC2000 accuracy (d) FVC2000 error rate (e) FVC2002 accuracy (f) FVC2002 error rate (g) FVC2004 accuracy (h) FVC2004 error rate

LR model in FVC2000 is a failure model, whereas it is a successful model here. The sensor type is the underlying cause of these variations in accuracy; moreover, the article suggests that the proposed LR model is considerable if the scanner is an analysis factor.

For resize level 25, most of the proposed method algorithms perform similarly to the classic method algorithm, with the difference being the error rate. From Figure 9 proposal identify

classical methods outperform the proposed method algorithm in some scenarios. When the NB algorithm fails on SD302 data, the proposed binary methods $MBNI_B$ and $MBSVNI_B$ achieve a 96% successive model. The traditional LR algorithm achieves successive scores, whereas the proposed method algorithm achieves the maximum point of the score. KNN accomplishes the maximum level of the score for FVC2000 data RF. When using the proposed binary method, NB improves the accuracy level. Except for FVC2000, the other datasets failed the DT algorithm the proposed DT performs well in FVC2000. The above discussion is based on Table 3 observations.

The current research scope of the proposed study is limited to the analysis of fingerprint images. In our study, various data sets were subjected to analysis. The results presented in this part instill a sense of belief within us. The strategies discussed in the related study mostly center around deep learning methodologies, as seen by the collective findings. Our primary objective is to enhance the performance of classical machine learning algorithms through the utilization of NS. The KNN model, as described, has superior performance compared to the other models discussed in the related work section. According to Adhinata [11], the maximum level of the score attainable by the KNN algorithm is 95%. However, the KNN model presented in this study achieved a perfect score of 100% through the utilization of machine learning methodologies. One notable benefit is its compatibility with both binary and self-intensity methodologies. The proposed project effectively implemented the LR and DT algorithms. In the study conducted by Kumar et al. [17], the best performance achieved was reported to be 96%. However, our research endeavors led to an enhancement in performance, resulting in a maximum achievement of 100%. Labati's [18] proposed NB algorithm achieves an accuracy rate of 52%. However, via our enhancements, we were able to significantly improve its performance, resulting in an accuracy rate of 89%. The proposal effectively improves the performance of machine learning algorithms. The classical technique column in Table 3 presents the methodology used by an ordinary machine learning algorithm.

5. **Conclusion**

This article proposes four new neutrosophic methods to classify fingerprint images. Furthermore, the hyperparameters is determined in order to classify the supervised algorithm. Our primary goal is to achieve the classification of fingerprint images without an individual's assistance. This technique allows researchers to classify fingerprint images for four different datasets without explicitly parameterizing the images. While low-range algorithms demonstrate LR accuracy of 5%, DT accuracy of 8%, and NB accuracy of 58%, high-range algorithms achieve LR accuracy of 5% and NB accuracy of 56%. However, alternative proposed method algorithms achieve higher levels of accuracy with a lower error rate. The proposal makes a significant

improvement in the classification performance of the images. This technique will support us in automated, supervised classification in the manner of an AI system. This strategy will be applied in features to unsupervised and other supervised algorithms as well as, if possible, other applications. This article claims that the proposed method's first step will further impact the field of digital images and accomplish desired aims. In order to decide on pixel values and attempt to improve performance in the future, there is also a research gap. As part of our feature work, we will extend this concept to object recognition and other types of image data.

Funding: This research received no external funding.
Acknowledgments: We would like to thank the Reviewers for investing in the necessary time and effort to evaluate the manuscript. We are grateful for all the insightful comments and suggestions that helped us enhance the quality of the manuscript.
Conflicts of Interest: The authors declare no conflict of interest.

References

1. Guo, Y., Cheng, H.D. and Zhang, Y., A new neutrosophic approach to image denoising. New Mathematics and Natural Computation, 5(03), pp.653-662, 2009.
2. Smarandache, F., Neutrosophy: neutrosophic probability, set, and logic: analytic synthesis & synthetic analysis, ,1998.
3. Smarandache, F., Multispace & Multistructure. Neutrosophic Transdisciplinarity (100 Collected Papers of Sciences), Vol. IV, 2010.
4. Abdel-Basset, M., Gamal, A., Hezam, I. M., & Sallam, K. M. (2023). An Effective Analysis of Risk Assessment and Mitigation Strategies of Photovoltaic Power Plants Based on Real Data: Strategies, Challenges, Perspectives, and Sustainability. International Journal of Energy Research, 2023.
5. Afzal, U., & Aslam, M. (2023). New Statistical Methodology for Capacitor Data Analysis via LCR Meter. Neutrosophic Systems with Applications, 8, 26-34.
6. Uma, G., & Nandhitha, S. (2023). An Investigative Study on Quick Switching System using Fuzzy and Neutrosophic Poisson Distribution. Neutrosophic Systems with Applications, 7, 61-70.
7. Heidari, H. and Chalechale, A., A new biometric identity recognition system based on a combination of superior features in finger knuckle print images. Turkish Journal of Electrical Engineering and Computer Sciences, 28(1), pp.238-252, 2020.
8. Mohammed, N.F., Jawad, M.J. and Ali, S.A., Biometric-based medical watermarking system for verifying privacy and source authentication. Kuwait Journal of Science, 47(3), 2020.
9. Tlhoolebe, J. and Dai, B., Object Selection as a Biometric. Entropy, 24(2), p.148, 2022.
10. Rish, I., An empirical study of the naive Bayes classifier. In IJCAI 2001 workshop on empirical methods in artificial intelligence (Vol. 3, No. 22, pp. 41-46), 2001, August.
11. Adhinata, F. and Junaidi, A., Gender Classification on Video Using FaceNet Algorithm and Supervised Machine Learning. International Journal of Computing and Digital Systems, 11(1), pp.199-208, 2022.
12. Quinlan, J.R., Induction of decision trees. Machine learning, 1, pp.81-106,1986.
13. Kruti, R., Patil, A. and Gornale, S.S., Fusion of local binary pattern and local phase quantization features set for gender classification using fingerprints. International Journal of Computer Sciences and Engineering, 7(1), pp.22-29, 2019.

14. Nguyen, H.T. and Nguyen, L.T., Fingerprints classification through image analysis and machine learning method. Algorithms, 12(11), p.241, 2019.
15. Breiman, L., Random forests. Machine learning, 45, pp.5-32, 2001.
16. Noor, K., Jan, T., Basheri, M., Ali, A., Khalil, R.A., Zafar, M.H., Ashraf, M., Babar, M.I. and Shah, S.W., Performances enhancement of fingerprint recognition system using classifiers. IEEE Access, 7, pp.5760-5768, 2018.
17. Kumar, M. and Kumar, D., An efficient gravitational search decision forest approach for fingerprint recognition. Kuwait Journal of Science, 50(2A), 2023.
18. Labati, R. D., Genovese, A., Munoz, E., Piuri, V., & Scotti, F. (2018). A novel pore extraction method for heterogeneous fingerprint images using convolutional neural networks. Pattern Recognition Letters, 113, 58-66.
19. Jang, H. U., Kim, D., Mun, S. M., Choi, S., & Lee, H. K. (2017). DeepPore: Fingerprint pore extraction using deep convolutional neural networks. IEEE signal processing Letters, 24(12), 1808-1812.
20. Jeon, W. S., & Rhee, S. Y. (2017). Fingerprint pattern classification using convolution neural network. International Journal of Fuzzy Logic and Intelligent Systems, 17(3), 170-176.
21. Saeed, F., Hussain, M., & Aboalsamh, H. A. (2022). Automatic fingerprint classification using deep learning technology (DeepFKTNet). Mathematics, 10(8), 1285.
22. Nahar, P., Chaudhari, N. S., & Tanwani, S. K. (2022). Fingerprint classification system using CNN. Multimedia Tools and Applications, 81(17), 24515-24527.
23. Walhazi, H., Maalej, A., & Amara, N. E. B. (2023). A multi-classifier system for automatic fingerprint classification using transfer learning and majority voting. Multimedia Tools and Applications, 1-24.
24. Dhatchinamoorthy, V. and Devarasan, E., 2023. An Analysis of Global and Adaptive Thresholding for Biometric Images Based on Neutrosophic Overset and Underset Approaches. Symmetry, 15(5), p.1102.
25. Pedregosa, F., Varoquaux, G., Gramfort, A., Michel, V., Thirion, B., Grisel, O., Blondel, M., Prettenhofer, P., Weiss, R., Dubourg, V. and Vanderplas, J., Scikit-learn: Machine learning in Python. the Journal of machine Learning research, 12, pp.2825-2830, 2011.
26. LaValley, M.P., Logistic regression. Circulation, 117(18), pp.2395-2399, 2008.
27. Maio, D., Maltoni, D., Cappelli, R., Wayman, J.L. and Jain, A.K., FVC2000: Fingerprint verification competition. IEEE transactions on pattern analysis and machine intelligence, 24(3), pp.402-412, 2002.
28. Maio, D., Maltoni, D., Cappelli, R., Wayman, J.L. and Jain, A.K., FVC2002: Second fingerprint verification competition. In 2002 International Conference on Pattern Recognition (Vol. 3, pp. 811-814). IEEE, 2002, August.
29. Maio, D., Maltoni, D., Cappelli, R., Wayman, J.L. and Jain, A.K., FVC2004: Third fingerprint verification competition. In Biometric Authentication: First International Conference, ICBA 2004, Hong Kong, China, July 15-17, 2004. Proceedings (pp. 1-7). Springer Berlin Heidelberg, 2004.
30. Fiumara, G.P., Flanagan, P.A., Grantham, J.D., Ko, K., Marshall, K., Schwarz, M., Tabassi, E., Woodgate, B. and Boehnen, C., NIST special database 302: Nail to nail fingerprint challenge, 2019.

Received: July 9, 2023. Accepted: Nov 20, 2023